



CHORUS

This is the accepted manuscript made available via CHORUS. The article has been published as:

Geometry of epitaxial GaAs/(Al,Ga)As quantum dots as seen by excitonic spectroscopy

Jun-Wei Luo and Alex Zunger

Phys. Rev. B **84**, 235317 — Published 28 December 2011

DOI: [10.1103/PhysRevB.84.235317](https://doi.org/10.1103/PhysRevB.84.235317)

Geometry of epitaxial GaAs/AlGaAs quantum dots as seen by excitonic spectroscopy

Jun-Wei Luo*

National Renewable Energy Laboratory, Golden, Colorado 80401, USA

Alex Zunger†

University of Colorado, Boulder, Colorado 80309, USA

(Dated: November 18, 2011)

It is shown that exciton and multi-exciton emission lines (“spectral barcode”) of a quantum dot conceal nontrivial structural information on the shape and size of the dot, information which can be uncovered by comparison with atomistic many-body theory. Application to the newly-established strain-free GaAs quantum dots grown via “droplet epitaxy” onto AlGaAs matrix reveal the shape and size as “seen” by spectroscopy. The results show that the previously determined dot height (~ 14 nm) as “seen” by cross-sectional scanning tunneling microscopy (XSTM) could not possibly be consistent with the excitonic signature (1.7-1.9 eV), as the latter must reflect a 1-4 nm tall dot. Multi-exciton “barcode” and fine structure spitting suggest GaAs/AlGaAs dots are in Gaussian-shape in agreement with XSTM measurement. Both spectroscopy and XSTM measurements were done on GaAs dots capped by the $\text{Al}_{0.3}\text{Ga}_{0.7}\text{As}$ barrier layer. The fact that XSTM sees tall dots and spectroscopy sees short dots is thus not because the dot change its height in one experiment relative to the other, but because different dots must have been used. This was uncovered by theoretical simulation of the experiment showing that the two experiments could not possibly correspond to the same dot.

PACS numbers: 78.67.-n, 68.65.Hb, 71.35.Pq

I. INTRODUCTION:

Molecular spectroscopy has always been intimately connected with molecular structure and symmetry through fundamental interpretative constructs such as symmetry-mandated selection-rules, level-degeneracies, and polarization¹. Yet, the spectroscopy of epitaxial semiconductor quantum dots (QDs) — large simple molecules made of $10^3 - 10^6$ atoms such as Si, InAs, or GaAs — has been largely conducted and interpreted without basic knowledge of the underlying structure. Indeed, the extremely rich (10-20 lines), high-resolution ($\sim 10 \mu\text{eV}$) single-dot excitonic spectra of such simple “macromolecules” being now measured almost routinely²⁻⁷ has not been accompanied by detailed structural information, other than cross-sectional scanning tunneling microscopy (XSTM) measurements^{8,9} which, however, can produce a range of diverging structures from the same measured relaxation profile on the same dot^{10,11}. Attempts to bridge this gap between spectra and structure have recently been made in the context of self-assembled (strained) In(Ga)As/GaAs dots by combining measured excitonic spectra with XSTM structural assessment of the same dot sample, using quantitative excitonic theory as the bridge. It was found¹⁰ that the calculated excitonic spectra produced by using as input a range of structural models offered by XSTM conflicted with the experimental spectra in a number of crucial aspects. However, a structure derived theoretically by matching the calculated spectra with experiment did agree with the basic data used to derive XSTM structural models (i.e., the measured outer relaxation profile of the cleaved dot). It was concluded that high resolution excitonic spectra contains significant structural information that can be unearthed using theory as a mining tool.

Until recently, epitaxial quantum dots were made mostly by a growth protocol (“Stranski-Krastanov”, or SK)^{3,4,12} requiring that the dot material have a significantly different lattice constant (generally larger) than the substrate on which it is grown, e.g., InAs-on-GaAs⁴ or InP-on-GaP¹². Lattice-matched material pairs such as GaAs on AlGaAs or InAs on GaSb were excluded until recently. The advent of “droplet epitaxy” growth mode¹³ (involving growth of cation-element droplets on a substrate and subsequently their crystallization into QDs by incorporation of the anion-element) has changed this, enabling epitaxial dots of lattice-matched pairs, thus opening a window to the understanding of the confinement physics of fundamental semiconductor material such as GaAs. The GaAs/AlGaAs dot is not just another SK dot system such as InAs/GaAs. Indeed, it is unstrained, and was grown by a completely different growth method (the molecular droplet epitaxy) rather than the gas-phase MBE used to grow InAs/GaAs. Furthermore, here GaAs is the dot whereas in InAs/GaAs the barrier is GaAs and the dot is InAs. Therefore, the conduction and valence band offsets (confinement potentials) in these two types of dots are different. Moreover, InAs and GaAs differ in bandgap, electron and hole effective masses and the relative positions of the conduction states at Γ, X, L . It is thus by no means obvious that there will be a similarity in the electronic structure results of GaAs/AlGaAs with InAs/GaAs. Indeed, the electronic structure we find is very different in a critical respect: the order of hole states. In GaAs/AlGaAs the light-hole (LH)-derived S-like state lies between two heavy-hole (HH)-derived

P-like hole states, whereas in InAs/GaAs the LH state is well below the HH-derived P-like hole states.

Recent XSTM measurement⁸ suggested that such QDs have Gaussian-shape instead of lens-shape as measured by Atomic force microscope (AFM)^{2,15-17} and dot height is around 14 nm^{8,15}. The measured exciton band gap by optical spectroscopy is about 1.7-1.9 eV^{2,17-20}. The present paper discusses the spectra *vs.* structure link for such QDs. We find that the GaAs QDs grown by droplet epitaxy approach indeed have Gaussian-shape as suggested by a recent XSTM measurement⁸. However, we find that dots as seen by optical spectroscopy are in 2-4 nm rather than XSTM determined value of 14 nm. AFM was not used but rather XSTM. Thus, the dots are all overgrown by a cap. The fact that XSTM sees tall dots and spectroscopy sees short dots is thus not because the dot change its height in one experiment relative to the other, but because different dots must have been used. This was uncovered by theoretical simulation of the experiment showing that the two experiments could not possibly correspond to the same dot.

II. METHOD OF CALCULATION

The one-particle states of a GaAs/AlGaAs QD are obtained by solving the Schrödinger equation of crystal (dot+matrix) potential $V(\mathbf{r})$ in a plane-wave basis set²¹. The screened potential $V(\mathbf{r})$ is described as a superposition of overlapping atomic (pseudo) potentials centered at the atomic positions: $V(\mathbf{r}) = \sum_n \sum_\alpha \hat{v}_\alpha(\mathbf{r} - \mathbf{R}_n - \mathbf{d}_\alpha)$, where $\hat{v}_\alpha(\mathbf{r} - \mathbf{R}_n - \mathbf{d}_\alpha)$ pertains to atom type α at site \mathbf{d}_α in the n th primary cell \mathbf{R}_n ²¹. Thus it forces upon eigenstates the correct atomically-resolved symmetry. The atomic potentials \hat{v}_α were empirically fit to experimental transition energies, effective masses, and deformation potentials of the bulk materials²¹. Specifically, fitted band gap is within 5 meV of the experimental value²¹. The (multi)exciton complexes are calculated using a configuration-interaction (CI) method²² in a basis set of Slater determinants $\{\Phi_{v,c}\}$ constructed from 16 electron and 16 hole (one-particle) states. The electron-hole (e-h) Coulomb interaction (binding the e-h pair and thus forming the exciton) and e-h exchange interaction (splitting symmetry-different exciton states) screened by a size-dependent screening function²² as well as correlations are introduced in CI.

III. RESULTS AND DISCUSSION

Measured Structure: GaAs/GaAlAs QDs grown by droplet epitaxy by Sakoda's group¹⁹ were initially described, on the basis of AFM measurements of uncapped QDs¹⁵, as being lens-shaped^{2,15-17} (schematic in left inset to Fig. 1), with averaged $[1\bar{1}0]$ -elongated base size of 70×50 nm (spread $\pm 10\%$) and dot height of 14 nm (spread $\pm 19\%$)¹⁵. Subsequent, more refined XSTM measurement of capped dots by Keizer *et. al.*⁸ of the dots grown by the same Sakoda's group^{15,19} showed instead a rather different, Gaussian shape (schematic in right inset to Fig. 1) with an average base size of 40 nm, height of 14 nm and a size distribution of 10 – 20%.

Spectra of single exciton: The measured spectroscopy^{2,17-20} of the QDs grown by the same Sakoda's group¹⁹ shows that the fundamental exciton emission from all kinds of spectroscopy measurements were in a range of 1.7-1.9 eV.

Calculated spectra for the measured structure leads to conflict with assumed structure: We have calculated the exciton gap energy of lens-shaped, Gaussian-shaped, and disk-shaped strain-free GaAs/AlGaAs QDs using our atomistic many-body pseudopotential method (Fig. 1). Notwithstanding the shape, the QDs having calculated exciton energy in the range of the experimental measured exciton energy of 1.7-1.9 eV are seen to have a much smaller dot height of only 1-4 nm compared to the experimentally stated value (~ 14 nm) by both AFM¹⁵ and XSTM⁸ approaches. This discrepancy, being well outside the measured size-distribution in the sample, indicates that the QDs measured by AFM or XSTM are not same as QDs seen by optical spectroscopy. We conclude²³ that the dot whose height was measured to be 14 nm in Refs. 8,15 is not the same dot used in Refs. 2,17-20 to measure the band gap and fine excitation structure. It is worth mentioning that the quantum dot height decreases from 14 nm when quantum dots are grown by droplet epitaxy on a (001)-oriented GaAs substrate⁸ to much smaller value of 2.3 ± 0.6 nm when quantum dots are grown on a (311)A-oriented GaAs substrate²⁴. However, the measurement of XSTM⁸ and spectroscopy^{2,17-20} considered in this paper, as well as theory, are all on (001) substrate.

Whereas to first order the magnitude of the excitonic emission energy reveals information mostly on the dot height, a more detailed measurement can also distinguish different dot shapes. We see from Fig. 1 that for the same base size and dot height, the lens-shaped QDs have an exciton gap energy that is smaller by as much as ~ 40 meV than that of Gaussian-shaped QDs, and that this is so in a wide range of dot heights of 1-12 nm. If droplet epitaxy grown GaAs/AlGaAs QDs are known to be either lens-shaped or Gaussian-shaped, this exciton shift is large enough to distinguish the QD shape if the base size, dot height, and exciton energy of optical spectroscopy seen QDs are accurately measured.

The shape of the dot as seen by the sequence of multi-exciton lines: Excitons in quantum dots can be created as neutral monoexciton X^0 having (1e,1h) or neutral biexciton XX^0 having (2e,2h), as well as charged excitons

such as positive trion X^+ with (1e,2h), negative trion X^- with (2e,1h), positive biexciton XX^+ with (2e,3h), and negative biexciton XX^- with (3e,2h), etc. Fig. 2 shows the calculated emission spectrum when a single electron-hole pair recombines within such multi-exciton complexes²⁵. The spectra consist of a few lines. Specially for XX^+ and XX^- we see several four and two lines, respectively, due to various S and P recombination channels and e-h exchange interaction induced fine-structure splitting (FSS) of multi-exciton complexes. This emission energy reflects both Coulomb and correlation interactions between all holes and electrons; these interactions ultimately reflect the overlap of the corresponding wave functions which is sensitive to the shape and size of the QD. Such complex and implicit dependences between the sequence of multi-exciton lines (“multi-exciton barcode”) and QD structure were used recently to decipher structural features from excitonic features. It was proposed²⁶ that such barcodes, consisting of X , X^+ , X^- , XX , XX^+ , XX^- , and X^{-2} lines can be correlated with geometrical features of the strained SK-grown InAs/GaAs QDs.

Here we will use this barcoding approach to unearth structural features of another class of dots based on unstrained, droplet epitaxy grown GaAs/GaAlAs. To do this we have calculated the sequence of multi-excitonic lines for a large number of dots covering three different basic shapes (lens shape, Gaussian shape, and disk-shape) and many structural parameters within these shapes (dot height, base size, shape anisotropy). Using this barcoding method, we can build a link between structure of strain-free GaAs/AlGaAs QDs and the excitonic emission spectrum. However, at present, the available experimentally measured excitonic emission spectrum of such dots includes only neutral monexciton X^0 , positive and negative trions X^+ and X^- , and neutral biexciton XX ^{02,17-20}. Figure 2 shows the atomistic calculated emission spectra (where we have aligned the energy of the monexciton X^0 lines) for lens-shaped [Fig. 2(a)] and Gaussian-shaped [Fig. 2(b)] QDs. In this partial excitonic emission spectrum, we find that the sequence of the following lines always obeys some “hard rules”²⁶,

$$X^- < XX^- < XX^0 < X^0. \quad (1)$$

The hard rules observed in all experimental spectra^{2,17-20} are that (i) both X^- and XX^0 are red shifted with respect to X^0 (i.e., have positive binding energies) (ii) the XX line always lies between X and X^- . Hard rule (iii)²⁶ related to X^{-2} has not been measured yet for GaAs/AlGaAs QDs. These three hard rules plus the position of X^0 line will provide the dot base size and height²⁶. From hard rules (i) and (ii) we estimate that the optical spectroscopy seen QDs has base size of 30-40 nm.

Interesting, we find that the positive trion (X^+) is related to the QD shape. Fig. 2(a) shows that in lens-shaped QDs the positive trion (X^+) of is always redshifted with respect to neutral monexciton (X^0). In contrast to lens-shaped QDs, in Gaussian-shaped QDs[Fig. 2(b)] the X^+ has a transition from redshift to blueshift when dot height decreases, in agreement with experimental measurements². Furthermore, our calculated transition point $E_{X^0} = 1.758$ eV also agrees with experimental value of 1.748 eV². Thus, we conclude that Gaussian-shape is more likely in droplet epitaxy grown GaAs/AlGaAs QDs.

FSS of mono-exciton vs QD shape. The FSS of an exciton^{25,27-29} refers to the splitting of the optical allowed (bright) exciton states due to both intrinsic crystal asymmetry as well as external shape anisotropy. The role of these two factors has been often confused in the literature^{17,19,20,30}, leading to the misuse of the FSS to infer shape anisotropy: In the Luttinger Hamiltonian representation the effective mass of hole is anisotropic in that its value along (100) is different from along (110). Thus, if one ignores the fact that the QDs under consideration are made of an atomistically-discrete materials, the symmetry of circular based dot in this Hamiltonian is C_{4v} . Despite this, numerous papers^{18,31} claimed that circular based lens shape dot has D_{2d} symmetry. This is because in a continuum approximation the [110] and $[1\bar{1}0]$ directions are equivalent. In such a D_{2d} symmetry, the four-fold degenerate exciton (originating from an electron of $J_z = \pm 1/2$ and a heavy-hole of $J_z = \pm 3/2$) splits into double-degenerate bright state (Γ_5) and two non-degenerate dark states (Γ_1 and Γ_2 , respectively). Because Γ_5 is degenerate in this approximation, the FSS is zero for cylindrically symmetric dots under the continuum point of view.

To account for the observed nonzero FSS, the continuum theory assumes that the FSS originates, in its entirety, from deviations from cylindrical symmetry^{17,19,20,30}. This shape anisotropy (e.g., elongation in $[1\bar{1}0]$ direction^{17,19,20}) of QD lowers then the D_{2d} symmetry to C_{2v} ³². The double-degenerate bright Γ_5 further splits into two non-degenerate states (Γ_2 and Γ_4). The lifting of the degeneracy of the two bright exciton states is referred to FSS and is used under the continuum point of view to fit the measured FSS into a geometric shape anisotropy.

In reality, the [110] and $[1\bar{1}0]$ directions are nonequivalent in zincblende crystal. This leads to the fact that even a QD having cylindrical shape already does not have the commonly thought D_{2d} symmetry, but is already lowered to C_{2v} , thus even a shape-symmetric dot has nonzero FSS. Although, this intrinsic crystal anisotropy was pointed out many times in atomistic theory^{27,33,34}, its contribution to FSS was always been neglected by the community^{17,19,20,30}. Fig. 3 shows the calculated atomistic many-body pseudopotential FSS for symmetric and asymmetric Gaussian-shaped QDs as well as symmetric lens-shaped QDs. In agreement with atomistic point view, we see that even the shape-symmetric Gaussian-shaped dot with base size of 30 nm has already a strong FSS ($\sim 30\mu\text{eV}$ for QDs having

exciton energy 1.7 eV) and that shape-asymmetry additionally adds some ($\sim 10\mu\text{eV}$) FSS. Whereas, the increase of base size for the shape-symmetric dots from 30 nm to 40 nm reduces the FSS by $\sim 20\mu\text{eV}$. Thus, attributing all of the FSS to shape asymmetry will greatly exaggerate the shape asymmetry.

It is most interesting to note that the slope of size-dependent FSS for both symmetric and asymmetric Gaussian-shaped QDs is opposite to the one seen in lens-shaped and in disk-shaped QDs. Specifically, the FSS of the Gaussian-shaped QDs decreases with increasing exciton emission energy (i.e, decreasing the dot height) in strong contrast to the case in lens-shaped and disk-shaped QDs where FSS increases with increasing exciton emission energy. We ascribe these two opposite size-dependent trends of FSS to two competitions: (i) FSS will be enhanced by quantum confinement effect due to increased overlapping of electron and hole wave functions; (ii) FSS will be washed out by random AlGaAs alloy distribution due to increased wave function leakage as decreasing the dot height. Because wave functions are expected to be more localized inside dot interior (at in-plane directions) in lens-shaped and disk-shaped QDs than in Gaussian-shaped QDs, the item (i) is dominantly in lens-shaped and disk-shaped QDs. However, in Gaussian-shaped QDs, item (i) and (ii) are comparable. These factors explain the observed opposite trends. The calculated size-dependent trend of FSS in Gaussian-shaped QDs is in excellent agreement with experimental measurement¹⁷. Thus, from the size-dependent trend of FSS we also suggest that droplet epitaxy grown GaAs/AlGaAs QDs are Gaussian-shape.

IV. SUMMARY

We show how the multi-exciton spectra of a droplet epitaxy QD encodes nontrivial structural information that can be uncovered by atomistic many-body pseudopotential calculation. We calculated single-particle energy levels, exciton gap, optical emission spectra, and FSS for a large number of strain-free GaAs/AlGaAs QDs with three different shapes and different structure parameters (base size, dot height, and shape anisotropy). From such multi-exciton complex emission spectrum and trend of size-dependent FSS we show that the droplet epitaxy strain-free GaAs/AlGaAs QDs are Gaussian-shape, in agreement with XSTM measurement, but the dot height as seen from optical spectroscopy measurements (exciton gap energy) are in 1-4 nm rather than ~ 14 nm as seen from XSTM measurement. This work promises that with increasing spectral resolution that would reveal even more multi-excitonic barcode lines, much detailed structural information could be revealed.

V. ACKNOWLEDGEMENTS

This work was funded by the U.S. Department of Energy, Office of Science, Basic Energy Science, Materials Sciences and Engineering, under Contract No. DE-AC36-08GO28308 to NREL.

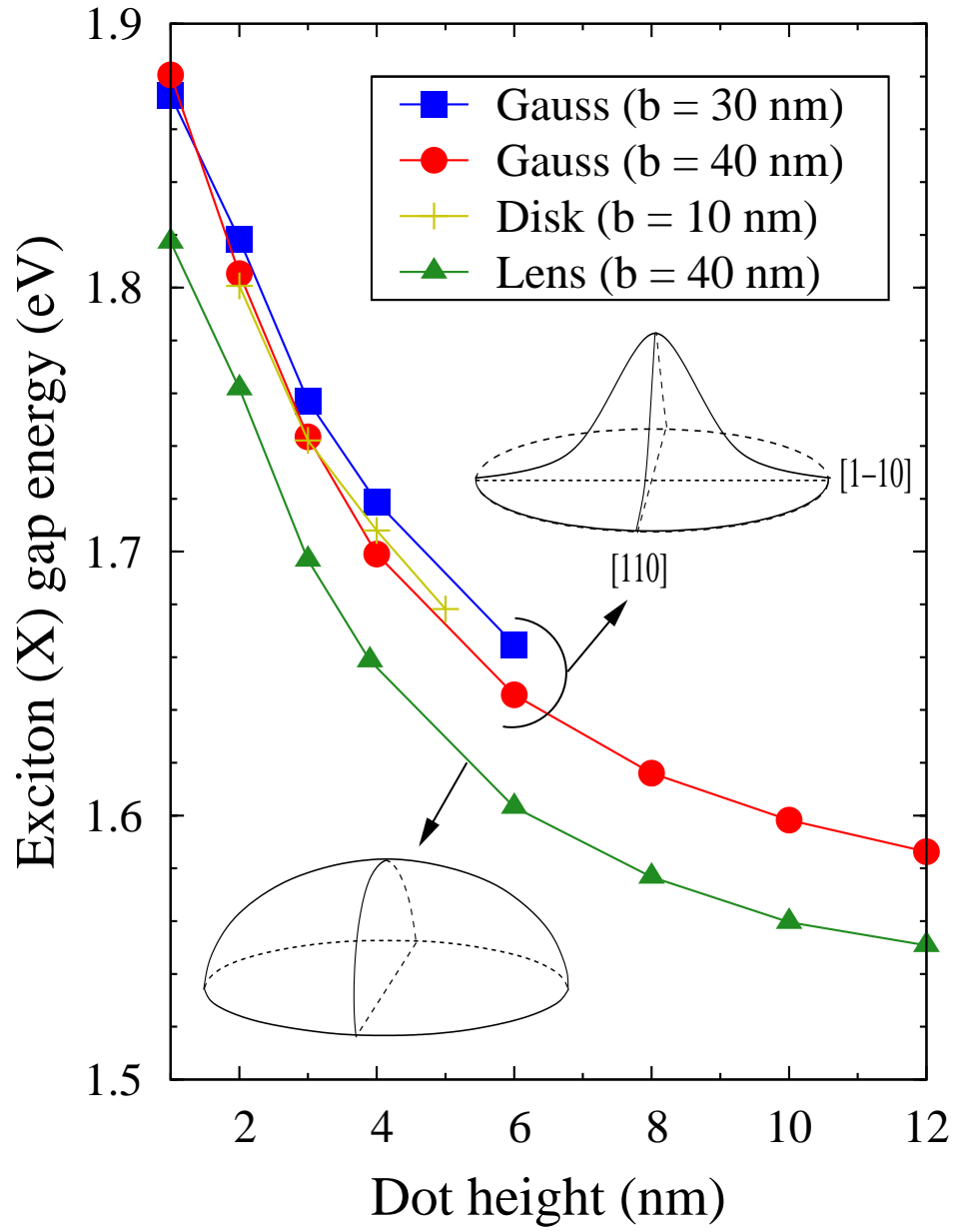


FIG. 1: Atomistic many-body pseudopotential calculated exciton emission energy of shape-symmetric Gaussian-shaped, lens-shaped, and disk-shaped GaAs/ $\text{Al}_{0.3}\text{Ga}_{0.7}\text{As}$ QDs (base size given in parentheses) as a function of dot height.

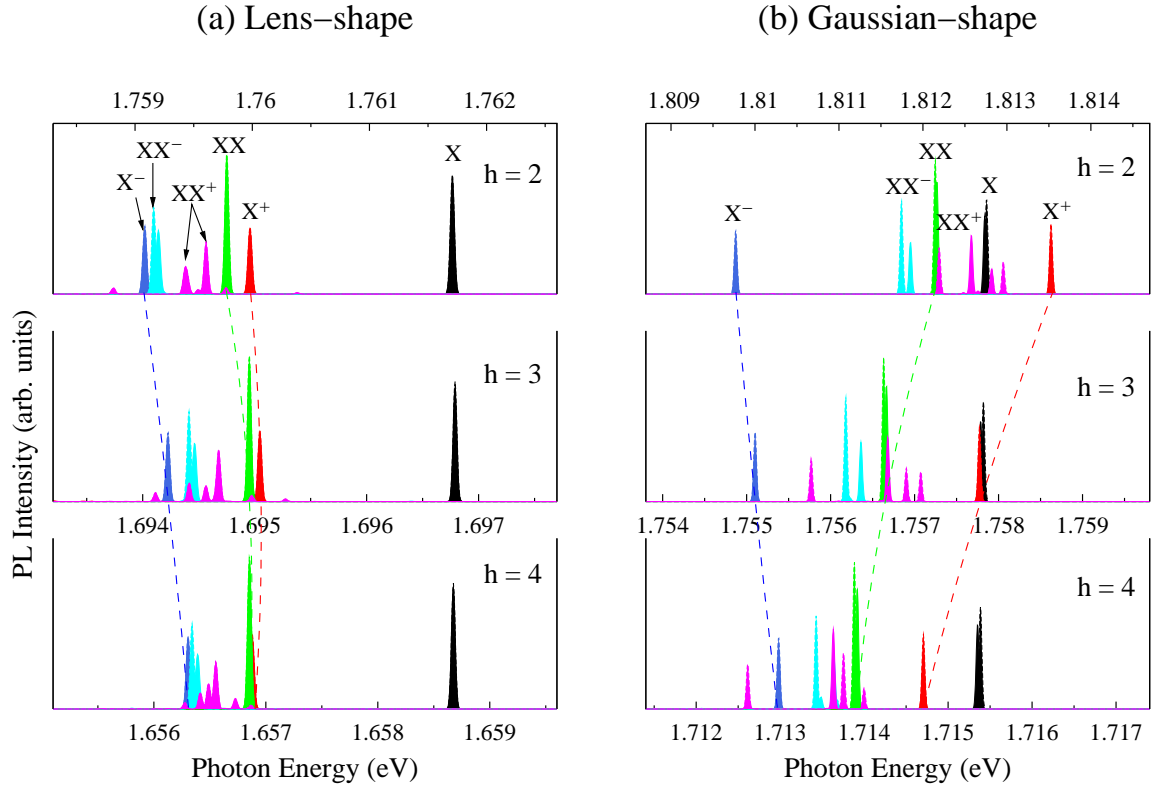


FIG. 2: Excitonic emission spectrum of (a) symmetric lens-shaped and (b) symmetric Gaussian-shaped GaAs/Al_{0.3}Ga_{0.7}As QDs with base size of $b = 40 \times 40$ nm and dot height $h = 2, 3,$ and 4 nm, respectively.

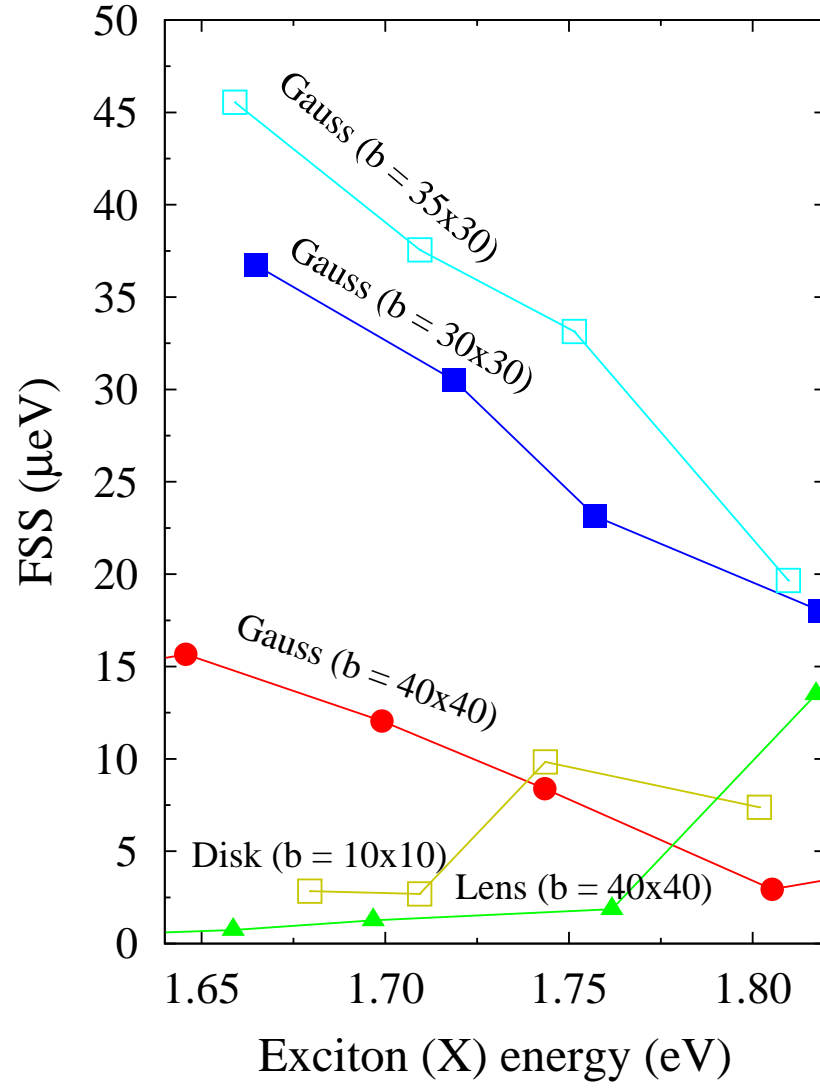


FIG. 3: FSS neutral mono-exciton of GaAs/AlGaAs QDs as a function of exciton emission energy (dot height) for different shapes (symmetric lens-shape, symmetric disk-shape, and symmetric and asymmetric Gaussian-shape) and base sizes (given in parentheses units in nm).

-
- * Electronic address: jun-wei.luo@nrel.gov
† Electronic address: alex.zunger@gmail.com
- ¹ G. M. Barrow, *Introduction to Molecular Spectroscopy* (McGraw-Hill, New York, 1962).
 - ² M. Abbarchi, T. Kuroda, T. Mano, K. Sakoda, C. A. Mastrandrea, A. Vinattieri, M. Gurioli, and T. Tsuchiya, Phys. Rev. B **82**, 201301(R) (2010).
 - ³ M. Ediger, G. Bester, A. Badolato, P.M. Petroff, K. Karrai, A. Zunger, and R.J. Warburton, Nat. Phys. **3**, 774 (2007).
 - ⁴ E. Poem, J. Shemesh, I. Marderfeld, D. Galushko, N. Akopian, D. Gershoni, B. D. Gerardot, A. Badolato, and P. M. Petroff, Phys. Rev. B **76**, 235304 (2007).
 - ⁵ I. Sychugov, R. Juhasz, J. Valenta, and J. Linnros, Phys. Rev. Lett. **94**, 087405 (2005).
 - ⁶ H. J. Krenner, E. C. Clark, T. Nakaoka, M. Bichler, C. Scheurer, G. Abstreiter, and J. J. Finley, Phys. Rev. Lett. **97**, 076403 (2006).
 - ⁷ P. Ester, S. Stuffer, S. M. de Vasconcellos, M. Bichler, and A. Zrenner, Phys. stat. sol. (c) **3**, 3722 (2006).
 - ⁸ J.G. Keizer, J. Bocquel, P.M. Koenraad, T. Mano, T. Noda, and K. Sakoda, Appl. Phys. Lett. **96**, 062101 (2010).
 - ⁹ J. H. Blokland, M. Bozkurt, J. M. Ulloa, D. Reuter, P. M. Koenraad, P. C. M. Christianen, and J. C. Maan, Appl. Phys. Lett. **94**, 023107 (2009).
 - ¹⁰ V. Mlinar, M. Bozkurt, J. M. Ulloa, M. Ediger, G. Bester, A. Badolato, P. M. Koenraad, R. J. Warburton, and A. Zunger, Phys. Rev. B **80**, 165425 (2009).
 - ¹¹ D.P. Kumah, S. Shusterman, Y. Paltiel, Y. Yacoby, and R. Clarke, Nat. nano. **4**, 835 (2009); D. P. Kumah, J. H. Wu, N. S. Husseini, V. D. Dasika, R. S. Goldman, Y. Yacoby, and R. Clarke, Appl. Phys. Lett. **98**, 021903 (2011). A more accurate structure profile of epitaxy QDs can be indirectly obtained from a full three-dimensional electron density map measured by a coherent Bragg rod analysis (COBRA) method.
 - ¹² F. Hatami, W. T. Masselink, L. Schrottke, J. W. Tomm, V. Talalaev, C. Kristukat, and A. R. Goñi, Phys. Rev. B **67**, 085306 (2003).
 - ¹³ N. Koguchi, S. Takahashi, T. Chikyow, J. Cryst. Growth **111**, 688 (1991); N. Koguchi and K. Ishige, Jpn. J. Appl. Phys., Part I **32**, 2052 (1993).
 - ¹⁴ K. Kowalik, O. Krebs, A. Lemaître, J. A. Gaj, and P. Voisin, Phys. Rev. B **77**, 161305(R) (2008).
 - ¹⁵ M. Jo, T. Mano, and K. Sakoda, J. Appl. Phys. **108**, 083505 (2010).
 - ¹⁶ K. Kuroda, T. Kuroda, K. Sakoda, K. Watanabe, N. Koguchi, and G. Kido, Appl. Phys. Lett. **88**, 124101 (2006).
 - ¹⁷ M. Abbarchi, C.A. Mastrandrea, T. Kuroda, T. Mano, K. Sakoda, N. Koguchi, S. Sanguinetti, V. Vinattieri, and M. Gurioli, Phys. Rev. B **78**, 125321 (2008).
 - ¹⁸ T. Belhadj, T. Amand, A. Kunold, C.-M. Simon, T. Kuroda, M. Abbarchi, T. Mano, K. Sakoda, S. Kunz, X. Marie, and B. Urbaszek, Appl. Phys. Lett. **97**, 051111 (2010).
 - ¹⁹ T. Mano, M. Abbarchi, T. Kuroda, C.A. Mastrandrea, A. Vinattieri, S. Sanguinetti, K. Sakoda, and M. Gurioli, Nanotechnology **20**, 395601 (2009).
 - ²⁰ M. Abbarchi, T. Kuroda, C. Mastrandrea, A. Vinattieri, S. Sanguinetti, T. Mano, K. Sakoda, M. Gurioli, Physica E **42**, 881 (2010).
 - ²¹ J.W. Luo, G. Bester, and A. Zunger, Phys. Rev. B **79**, 125329 (2009).
 - ²² A. Franceschetti, H. Fu, L. W. Wang, and A. Zunger, Phys. Rev. B **60**, 1819 (1999).
 - ²³ We are grateful to Prof. P.M. Koenraad and Dr. M. Takaaki for clarifying to us now that the dots used in XSTM were different than those used for PL measurements.
 - ²⁴ J. G. Keizer, M. Jo, T. Mano, T. Noda, K. Sakoda, and P. M. Koenraad, Appl. Phys. Lett. **98**, 193112 (2011).
 - ²⁵ V. Mlinar and A. Zunger, Phys. Rev. B **80**, 205311 (2009).
 - ²⁶ V. Mlinar and A. Zunger, Phys. Rev. B **80**, 035328 (2009).
 - ²⁷ E.L. Ivchenko, phys. stat. sol.(a) **164**, 487 (1997).
 - ²⁸ R. Singh and G. Bester, Phys. Rev. Lett. **104**, 196803 (2010).
 - ²⁹ J. W. Luo, A. Franceschetti, and A. Zunger, Phys. Rev. B **79**, 201301(R) (2009).
 - ³⁰ J.D. Plumhof, V. Křápek, L. Wang, A. Schliwa, D. Bimberg, A. Rastelli, and O.G. Schmidt, Phys. Rev. B **81**, 121309(R) (2010).
 - ³¹ M. Bayer, G. Ortner, O. Stern, A. Kuther, A. A. Gorbunov, A. Forchel, P. Hawrylak, S. Fafard, and K. Hinzer, T. L. Reinecke, S. N. Walck, J. P. Reithmaier, F. Klopff, and F. Schäfer, Phys. Rev. B **65**, 195315 (2002).
 - ³² If the center of dot base interface does not anchor on a common atom (namely As atom), then the symmetry of circular based dot is C_1 rather than C_{2v} . In C_1 group two bright exciton states belong to the same symmetry representation and thus they will couple if their energy are close enough (namely $FSS < 5\mu\text{eV}^{28}$). For dots with $FSS > 5\mu\text{eV}$, FSS is not sensitive to the choice of the dot base center.
 - ³³ G. Bester, S. Nair, and A. Zunger, Phys. Rev. B **67**, 161306(R) (2003).
 - ³⁴ C. Pryor, J. Kim, L. W. Wang, A. J. Williamson, and A. Zunger, J. Appl. Phys. **83**, 2548 (1998).